Tm-doped fiber laser mode-locked by graphene-polymer composite

M. Zhang,[1] E. J. R. Kelleher,[1,*] F. Torrisi,[2] Z. Sun,[2], T. Hasan,[2] D. Popa,[2] F. Wang,[2] A. C. Ferrari,[2] S. V. Popov,[1] and J. R. Taylor[1]

[1]*Femtosecond Optics Group, Department of Physics, Imperial College London, Prince Consort Road, London SW7 2BW, UK*

[2]*Department of Engineering, University of Cambridge, Cambridge, CB3 0FA, UK*

[*]*edmund.kelleher08@imperial.ac.uk*

Abstract: We demonstrate mode-locking of a thulium-doped fiber laser operating at 1.94 μm, using a graphene-polymer based saturable absorber. The laser outputs 3.6 ps pulses, with $\sim$0.4 nJ energy and an amplitude fluctuation $\sim$0.5%, at 6.46 MHz. This is a simple, low-cost, stable and convenient laser oscillator for applications where eye-safe and low-photon-energy light sources are required, such as sensing and biomedical diagnostics.

OCIS codes: (060.3510) Lasers, fiber; (140.4050) Mode-locked lasers; (320.7090) Ultrafast lasers; (160.4236) Nanomaterials.

References and links

1. L. E. Nelson, E. P. Ippen, and H. A. Haus, "Broadly tunable sub-500 fs pulses from an additive-pulse mode-locked thulium-doped fiber ring laser," Appl. Phys. Lett. **67**, 19–21 (1995).
2. R. C. Sharp, D. E. Spock, N. Pan, and J. Elliot, "190-fs passively mode-locked thulium fiber laser with a low threshold," Opt. Lett. **21**, 881–883 (1996).
3. S. Kivisto, T. Hakulinen, M. Guina, and O. G. Okhotnikov, "Tunable Raman Soliton Source Using Mode-Locked Tm-Ho Fiber Laser," IEEE Photon. Technol. Lett. **19**, 934–936 (2007).
4. M. A. Solodyankin, E. D. Obraztsova, A. S. Lobach, A. V. Tausenev, V. I. Konov, and E. M. Dianov, "Mode-locked 1.93 μm thulium fiber laser with a carbon nanotube absorber," Opt. Lett. **33**, 1336–1338 (2008).
5. Q. Wang, J. Geng, T. Luo, and S. Jiang, "Mode-locked 2 μm laser with highly thulium-doped silicate fiber," Opt. Lett. **34**, 3616–3618 (2009).
6. N. M. Fried and K. E. Murray, "New technologies in Endourology high-power thulium fiber laser ablation of urinary tissues at 1.94 μm," J. Endourol. **19**, 25-31 (2005).
7. S. Amini-Nik, D. Kraemer, M. L. Cowan, K. Gunaratne, P. Nadesan, B. A. Alman, and R. J. D. Miller, "Ultrafast Mid-IR Laser Scalpel: Protein Signals of the Fundamental Limits to Minimally Invasive Surgery," PLoS ONE, **5**, e13053 (2010).
8. W. Zeller, L. Naehle, P. Fuchs, F. Gerschuetz, L. Hildebrandt, and J. Koeth, "DFB Lasers Between 760 nm and 16 μm for Sensing Applications," Sensors **10**, 2492–2510 (2010).
9. B. Walsh, "Review of Tm and Ho materials; spectroscopy and lasers," Laser Phys. **19**, 855–866 (2009).
10. M. Ebrahim-Zadeh, I. T.Sorokina, *Mid-infrared Coherent Sources And Applications* (Springer, 2008).
11. F. G. Gebhardt, "High power laser propagation," Appl. Opt. **15**, 1479–1493 (1976).
12. M. E. Fermann and I. Hartl, "Ultrafast Fiber Laser Technology," IEEE J. Sel.Top. Quantum Electron.**15**,191–206(2009).
13. O. Okhotnikov, A. Grudinin, and M. Pessa, "Ultra-fast fibre laser systems based on SESAM technology: new horizons and applications," New J. Phys. **6**, 177 (2004).
14. U. Keller, "Recent developments in compact ultrafast lasers," Nature **424**, 831–838 (2003).
15. Y.-C. Chen, N. R. Raravikar, L. S. Schadler, P. M. Ajayan,G.-C. Wang, and X.-C. Zhang, "Ultrafast optical switching properties of single-wall carbon nanotube polymer composites at 1.55um," Appl. Phys. Lett. **81**, 975–977 (2002).
16. M. Breusing, C. Ropers, and T. Elsaesser, "Ultrafast Carrier Dynamics in Graphite," Phys. Rev. Lett. **102**, 086809 (2009).

#172887 - $15.00 USD Received 18 Jul 2012; revised 28 Aug 2012; accepted 29 Aug 2012; published 18 Oct 2012

17. D. Brida, C. Manzoni, G. Cerullo, A. Tomadin, M. Polini, R. R. Nair, A. K. Geim, K. S. Novoselov, S. Milana, A. Lombardo, and A. C. Ferrari, in Proceedings of Quantum Electronics and Laser Science Conference (QELS), San Jose, California (OSA, 2012), paper QTh3H.1.
18. F. Wang, A. G. Rozhin, V. Scardaci, Z. Sun, F. Hennrich, I. H. White, W. I. Milne, and A. C. Ferrari, "Wideband-tuneable, nanotube mode-locked, fibre laser," Nat. Nanotechnol. **3**, 738–742 (2008).
19. Z. Sun, D. Popa, T. Hasan, F. Torrisi, F. Wang, E. Kelleher, J. Travers, V. Nicolosi, and A. Ferrari, "A stable, wideband tunable, near transform-limited, graphene-mode-locked, ultrafast laser," Nano Res. **3**, 653–660 (2010).
20. D. Popa, Z. Sun, T. Hasan, F. Torrisi, F. Wang, and A. C. Ferrari, "Graphene Q-switched, tunable fiber laser," Appl. Phys. Lett. **98**, 073106 (2011).
21. T. Hasan, Z. Sun, F. Wang, F. Bonaccorso, P. H. Tan, A. G. Rozhin, and A. C. Ferrari, "Nanotube-Polymer Composites for Ultrafast Photonics," Adv. Mater. **21**, 3874–3899 (2009).
22. F. Bonaccorso, Z. Sun, T. Hasan, and A. C. Ferrari, "Graphene Photonics and Optoelectronics," Nat. Photonics **4**, 611–622 (2010).
23. Z. Sun, T. Hasan, F. Torrisi, D. Popa, G. Privitera, F. Wang, F. Bonaccorso, D. M. Basko, and A. C. Ferrari, "Graphene Mode-Locked Ultrafast Laser," ACS Nano **4**, 803–810 (2010).
24. S. Y. Set, H. Yaguchi, Y. Tanaka, and M. Jablonski, "Ultrafast fiber pulsed lasers incorporating carbon nanotubes," IEEE J. Sel. Top. Quantum Electron. **10**, 137–146 (2004).
25. V. Scardaci, Z. Sun, F. Wang, A. G. Rozhin, T. Hasan, F. Hennrich, I. H. White, W. I. Milne, and A. C. Ferrari, "Carbon Nanotube Polycarbonate Composites for Ultrafast Lasers," Adv. Mater. **20**, 4040–4043 (2008).
26. E. J. R. Kelleher, J. C. Travers, E. P. Ippen, Z. Sun, A. C. Ferrari, S. V. Popov, and J. R. Taylor, "Generation and direct measurement of giant chirp in a passively mode-locked laser," Opt. Lett. **34**, 3526–3528 (2009).
27. Z. Sun, A. G. Rozhin, F. Wang, V. Scardaci, W. I. Milne, I. H. White, F. Hennrich, and A. C. Ferrari, "L-band ultrafast fiber laser mode locked by carbon nanotubes," Appl. Phys. Lett. **93**, 061114 (2008).
28. Z. Sun, A. G. Rozhin, F. Wang, T. Hasan, D. Popa, W. O'Neill, and A. C. Ferrari, "A compact, high power, ultrafast laser mode-locked by carbon nanotubes," Appl. Phys. Lett. **95**, 253102 (2009).
29. Z. Sun, T. Hasan, F. Wang, A. G. Rozhin, I. H. White, and A. C. Ferrari, "Ultrafast Stretched-Pulse Fiber Laser Mode-Locked by Carbon Nanotubes," Nano Res. **3**, 404–411 (2010).
30. G. Della Valle, R. Osellame, G. Galzerano, N. Chiodo, G. Cerullo, P. Laporta, O. Svelto, U. Morgner, A. G. Rozhin, V. Scardaci, and A. C. Ferrari, "Passive mode locking by carbon nanotubes in a femtosecond laser written waveguide laser," Appl. Phys. Lett. **89**, 231115 (2006).
31. S. J. Beecher, R. R. Thomson, N. D. Psaila, Z. Sun, T. Hasan, A. G. Rozhin, A. C. Ferrari, and A. K. Kar, "320 fs pulse generation from an ultrafast laser inscribed waveguide laser mode-locked by a nanotube saturable absorber," Appl. Phys. Lett. **97**, 111114 (2010).
32. T. R. Schibli, K. Minoshima, H. Kataura, E. Itoga, N. Minami, S. Kazaoui, K. Miyashita, M. Tokumoto, and Y. Sakakibara, "Ultrashort pulse-generation by saturable absorber mirrors based on polymer-embedded carbon nanotubes," Opt. Express **13**, 8025–8031 (2005).
33. A. Schmidt, S. Rivier, G. Steinmeyer, J. H. Yim, W. B. Cho, S. Lee, F. Rotermund, M. C. Pujol, X. Mateos, M. Aguilo, F. Diaz, V. Petrov, and U. Griebner, "Passive mode locking of Yb:KLuW using a single-walled carbon nanotube saturable absorber," Opt. Lett. **33**, 729–731 (2008).
34. P. A. Obraztsov, A. A. Sirotkin, E. D. Obraztsova, Y. P. Svirko, and S. V. Garnov, "Carbon-Nanotube-Based Saturable Absorbers for Near Infrared Solid State Lasers," Opt. Rev. **17**, 290–293 (2010).
35. Y. W. Song, S. Yamashita, C. S. Goh, and S. Y. Set, "Passively mode-locked lasers with 17.2 GHz fundamental-mode repetition rate pulsed by carbon nanotubes," Opt. Lett. **32**, 430–432 (2007).
36. I. H. Baek, H. W. Lee, S. Bae, B. H. Hong, Y. H. Ahn, D.-I. Yeom, and F. Rotermund, "Efficient Mode-Locking of Sub-70-fs Ti:Sapphire Laser by Graphene Saturable Absorber," Appl. Phys. Express **5**, 032701 (2012).
37. W. D. Tan, C. Y. Su, R. J. Knize, G. Q. Xie, L. J. Li, and D. Y. Tang, "Mode locking of ceramic Nd:YAG with graphene as a saturable absorber," Appl. Phys. Lett. **96**, 031106 (2010).
38. W. B. Cho, J. H. Yim, S. Y. Choi, S. Lee, U. Griebner, V. Petrov, and F. Rotermund, "Mode-locked self-starting Cr:forsterite laser using a single-walled carbon nanotube saturable absorber," Opt. Lett. **33**, 2449–2451 (2008).
39. A. Martinez, K. Fuse, B. Xu, and S. Yamashita, "Optical deposition of graphene and carbon nanotubes in a fiber ferrule for passive modelocked lasing", Opt. Express **18**, 23054–23061 (2010).
40. D. Popa, Z. Sun, F. Torrisi, T. Hasan, F. Wang, and A. C. Ferrari, "Sub 200 fs pulse generation from a graphene mode-locked fiber laser," Appl. Phys. Lett. **97**, 203106 (2010).
41. J. Liu, Y. G. Wang, Z. S. Qu, L. H. Zheng, L. B. Su, and J. Xu, "Graphene oxide absorber for 2 μm passive mode-locking Tm:YAlO3 laser," Laser Phys. Lett. **9**, 15–19 (2012).
42. J. Ma, G. Q. Xie, P. Lv, W. L. Gao, P. Yuan, L. J. Qian, H. H. Yu, H. J. Zhang, J. Y. Wang, and D. Y. Tang, "Graphene mode-locked femtosecond laser at 2 μm wavelength," Opt. Lett. **37**, 2085–2087 (2012).
43. S. Stankovich, D. A. Dikin, G. H. B. Dommett, K. M. Kohlhaas, E. J. Zimney, E. A. Stach, R. D. Piner, S. T. Nguyen, and R. S. Ruoff, "Graphene-based composite materials," Nature **442**, 282–286 (2006).
44. C. Mattevi, G. Eda, S. Agnoli, S. Miller, K. A. Mkhoyan, O. Celik, D. Mostrogiovanni, G. Granozzi, E. Garfunkel, and M. Chhowalla, "Evolution of Electrical, Chemical, and Structural Properties of Transparent and Conducting Chemically Derived Graphene Thin Films," Adv. Funct. Mater. **19**, 2577–2583 (2009).

#172887 - $15.00 USD Received 18 Jul 2012; revised 28 Aug 2012; accepted 29 Aug 2012; published 18 Oct 2012

45. X. Li, W. Cai, J. An, S. Kim, J. Nah, I. Jung, E. Tutuc, S. K. Banerjee, L. Colombo, and R. S. Ruoff, "Large-Area Synthesis of High-Quality and Uniform Graphene Films on Copper Foils," Science **324**,1312–1314(2009).
46. K. S. Kim, Y. Zhao, H. Jang, S. Y. Lee, J. M. Kim, K. S. Kim, J.-H. Ahn, P. Kim, J.-Y. Choi, and B. H. Hong, "Large-scale pattern growth of graphene films for stretchable transparent electrodes," Nature **457**, 706–710 (2009).
47. Y. Hernandez, V. Nicolosi, M. Lotya, F. M. Blighe, Z. Y. Sun, S. De, I. T. McGovern, B. Holland, M. Byrne, Y. K. Gunko, J. J. Boland, P. Niraj, G. Duesberg, S. Krishnamurthy, R. Goodhue, J. Hutchison, V. Scardaci, A. C. Ferrari, and J. N. Coleman, "High-yield production of graphene by liquid-phase exfoliation of graphite," Nat. Nanotechnol. **3**, 563–568 (2008).
48. S. Bae, H. Kim, Y. Lee, X. Xu, J.-S. Park, Y. Zheng, J. Balakrishnan, T. Lei, H. Ri Kim, Y. I. Song, Y.-J. Kim, K. S. Kim, B. Ozyilmaz, J.-H. Ahn, B. H. Hong, and S. Iijima, "Roll-to-roll production of 30 inch graphene films for transparent electrodes," Nat. Nanotechnol. **5**, 574–578 (2010).
49. C. Berger, Z. Song, T. Li, X. Li, A. Y. Ogbazghi, R. Feng, Z. Dai, A. N. Marchenkov, E. H. Conrad, P. N. First, and W. A. de Heer, "Ultrathin Epitaxial Graphite: 2D Electron Gas Properties and a Route toward Graphene-based Nanoelectronics," J. Phys. Chem. B **108**, 19912–19916 (2004).
50. P. W. Sutter, J.-I. Flege, and E. A. Sutter, "Epitaxial graphene on ruthenium," Nat. Mater. **7**, 406–411 (2008).
51. J.S.Wu,W.Pisula,and K.Mullen, "Graphenes as potential material for electronics," Chem. Rev.**107**,718–747(2007).
52. A. C. Ferrari, J. C. Meyer, V. Scardaci, C. Casiraghi, M. Lazzeri, F. Mauri, S. Piscanec, D. Jiang, K. S. Novoselov, S. Roth, and A. K. Geim, "Raman Spectrum of Graphene and Graphene Layers," Phys. Rev. Lett. **97**, 187401 (2006).
53. A. C. Ferrari, and J. Robertson, "Interpretation of Raman spectra of disordered and amorphous carbon," Phys. Rev. B **61**, 14095–14107 (2000).
54. C. Casiraghi, A. Hartschuh, H. Qian, S. Piscanec, C. Georgi, A. Fasoli, K. S. Novoselov, D. M. Basko, and A. C. Ferrari, "Raman Spectroscopy of Graphene Edges," Nano Lett. **9**, 1433–1441 (2009).
55. A. C. Ferrari, and J. Robertson, "Resonant Raman spectroscopy of disordered, amorphous, and diamondlike carbon," Phys. Rev. B **64**, 075414 (2001).
56. L. G. Cancado, A. Jorio, E. H. M. Ferreira, F. Stavale, C. A. Achete, R. B. Capaz, M. V. O. Moutinho, A. Lombardo, T. S. Kulmala, and A. C. Ferrari, "Quantifying Defects in Graphene via Raman Spectroscopy at Different Excitation Energies," Nano Lett. **11**, 3190–3196 (2011).
57. S. Latil, V. Meunier, and L. Henrard, "Massless fermions in multilayer graphitic systems with misoriented layers: Ab initio calculations and experimental fingerprints," Phys. Rev. B **76**, 201402 (2007).
58. V. G. Kravets, A. N. Grigorenko, P. Blake, S. Anissimova, K. S. Novoselov, and A. K. Geim, "Spectroscopic ellipsometry of graphene and an exciton-shifted van Hove peak in absorption," Phys. Rev. B **81**, 155413 (2010).
59. H. C. Haas, H. Husek, and L. D. Taylor, "On the ultraviolet absorption spectrum of polyvinyl alcohol," Journal of Polymer Science Part A: General Papers **1**, 1215–1226 (1963).
60. R. R. Nair, P. Blake, A. N. Grigorenko, K. S. Novoselov, T. J. Booth, T. Stauber, N. M. R. Peres, and A. K. Geim, "Fine Structure Constant Defines Visual Transparency of Graphene," Science **320**, 1308–1308 (2008).
61. G. P. Agrawal, *Applications of Nonlinear Fiber Optics*. (Academic Press, 2001).
62. D. Von der Linde, "Characterization of the Noise in Continuously Operating Mode-Locked Lasers," Appl. Phys. B **39**, 201–217 (1986).
63. D. Turchinovich, X. M. Liu, and J. Laegsgaard, "Monolithic all-PM femtosecond Yb-fiber laser stabilized with a narrow-band fiber Bragg grating and pulse-compressed in a hollow-core photonic crystal fiber," Opt. Express **16**, 14004–14014 (2008).

1. Introduction

Ultrafast lasers based on thulium (Tm) doped fibers [1–5], operating in the $\sim$2 μm range, are important to address demands for mid-IR sources necessary for a variety of applications, ranging from molecular spectroscopy and biomedical diagnostics, to medicine [6] and remote sensing [7]. The 2 μm region is important because several gas molecules (e.g. CO_2 [8]) have characteristic absorption lines. Since liquid water (main constituent of human tissue) absorbs more strongly at $\sim$2 μm ($\sim$100 cm^{-1}) than at $\sim$1.5 μm ($\sim$10 cm^{-1}) and $\sim$1 μm ($\sim$1 cm^{-1}), $\sim$2 μm laser sources are promising for medical diagnostic and laser surgery [9]. In addition, Light Detection And Ranging (LIDAR) [10] measurements and optical free-space telecommunications [10] can be performed within the 2–2.5 μm atmospheric transparency window [11]. Furthermore, fiber lasers offer advantages compared to solid-state lasers, such as compact geometry, efficient heat dissipation and alignment-free operation [12, 13].

2 μm fiber lasers have been mainly mode-locked using nonlinear polarization evolution

#172887 - $15.00 USD Received 18 Jul 2012; revised 28 Aug 2012; accepted 29 Aug 2012; published 18 Oct 2012

(NPE) [1] and semiconductor saturable absorber mirrors (SESAMs) [3]. However, these have disadvantages: NPE suffers from bulky construction and environmental sensitivity [1], SESAMs have complex fabrication and packaging and as well as limited bandwidth [14]. Nanotubes and graphene are promising saturable absorbers (SA) due to their favorable properties: ultrafast recovery time [15–17], broadband operation [18, 19], ease of fabrication [18–22] and integration [21, 22] into all-fiber configurations. While, broadband operation can be achieved using a distribution of nanotube diameters [18], this is an intrinsic property of graphene due to the gapless linear dispersion of Dirac electrons [19, 20, 22, 23]. Nanotubes have mode-locked fiber [18, 24–29], waveguide [30, 31], solid-state [32–34] and semiconductor lasers [35], covering from $\sim$0.8 to $\sim$2 μm [21, 22]. Ultrafast pulse generation at 0.8 [36], 1 [37], 1.3 [38] and 1.5 μm [19, 21–23, 39, 40] was demonstrated by exploiting graphene saturable absorbers (GSAs). Refs. [41, 42] reported 2 μm solid-state lasers mode-locked with graphene oxide and chemical vapor deposited (CVD) 1–2 layer graphene. Graphene oxide [43, 44] is fundamentally different from graphene: it is an insulating material with a mixture of sp^2/sp^3 regions [43, 44], with lots of defects and gap states [44]. Thus, it does not offer in principle the wideband tunability of graphene. CVD graphene, on the other hand, is normally grown at very high temperature on Cu [45] or Ni substrate [46]. Therefore, extra steps are required to transfer graphene to the target substrates for photonic applications. Indeed, graphene can be produced in a variety of ways, ranging from micromechanical cleavage [22], to liquid phase exfoliation (LPE) [47], CVD of hydrocarbons [45, 48], carbon segregation from silicon carbide [49] or metal substrates [50] and chemical synthesis from polyaromatic hydrocarbons [51]. LPE has the advantage of scalability, room temperature processing, and does not require any growth substrate. This produces dispersions that can be easily embedded into polymers to form composites with novel optoelectronic properties to be integrated into various systems [22].

Here, we demonstrate a fiber laser mode-locked using a graphene-polymer composite. It operates at 1.94 μm, with low-noise 3.6 ps pulses. Our results show the potential of GSAs for practical fiber lasers in the mid-IR.

2. Device fabrication and characterization

The graphene-polymer composite is produced as follows: 120 mg of graphite (NGS, Naturgraphit) and 90 mg of sodium deoxycholate (SDC) are sonicated at room temperature. The unexfoliated particles are allowed to settle for 10 minutes, followed by 60 minutes of centrifugation at $\sim$17000 g. The top 70% of the centrifuged dispersion is then used for the composite fabrication. Drops are also placed on Transmission Electron Microscope (TEM) grids for analysis in a high resolution TEM (HRTEM). Combined HRTEM and normal-incidence/tilted angle electron diffraction measurements show that our dispersion has $\sim$66% $\leq$ 3-layer flakes ($\sim$26% single layer, $\sim$22% bi-layer and $\sim$18% tri-layer). The remainder have less than 10 layers. The dispersion is also drop-cast on Si/SiO_2 for Raman measurements with a Renishaw 1000. 5 ml of dispersion is then mixed with polyvinyl alcohol (PVA) in water ($\sim$2 wt%) and centrifuged at $\sim$4000 g. Evaporation at room temperature gives a $\sim$40 μm film; finally, further Raman and absorption measurements are performed.

Figure 1 plots a typical Raman spectrum of a flake deposited on Si/SiO_2. Besides the G and 2D peaks, this has significant D and D$'$ intensities [52, 53]. We assign the D and D$'$ peaks to the edges of the submicrometer flakes, rather than a large amount of disorder within the flakes [54]. This is further supported by analyzing the G peak dispersion, Disp(G). In disordered carbons the G peak position, Pos(G), increases with decreasing excitation wavelength, from IR to UV [53]. Thus, Disp(G)$= \Delta Pos(G)/\Delta\lambda_L$, where λ_L is the laser excitation wavelength, increases with disorder [53, 55]. FWHM(G) always increases with disorder [56]. Hence, combining the intensity ratio of the D and G peaks, I(D)/I(G), with FWHM(G) and Disp(G) al-

#172887 - $15.00 USD Received 18 Jul 2012; revised 28 Aug 2012; accepted 29 Aug 2012; published 18 Oct 2012

lows us to discriminate between edges, and disorder in the bulk of the samples. In the latter case, a higher I(D)/I(G) would correspond to higher FWHM(G) and Disp(G). By analyzing 30 flakes, we find that the distribution of Disp(G), I(D)/I(G) and FWHM(G) are not correlated, indicating that the D peak is mostly due to edges. Also, Disp(G) is nearly zero for all samples (compared to $\geq$0.1 cm^{-1} nm^{-1} expected for disordered carbons [55]). Although 2D is broader than in pristine graphene, it is still a single Lorentzian. This implies that even if the flakes are multilayers, they are electronically decoupled and, to a first approximation, behave as a collection of single layers [57]. Figure 1 compares a typical flake with our graphene-PVA composite and pure PVA. We note that the spectrum of the composite (Fig. 1) is a superposition of that of the flake and PVA . Thus, PVA does not affect the structure of the embedded flakes.

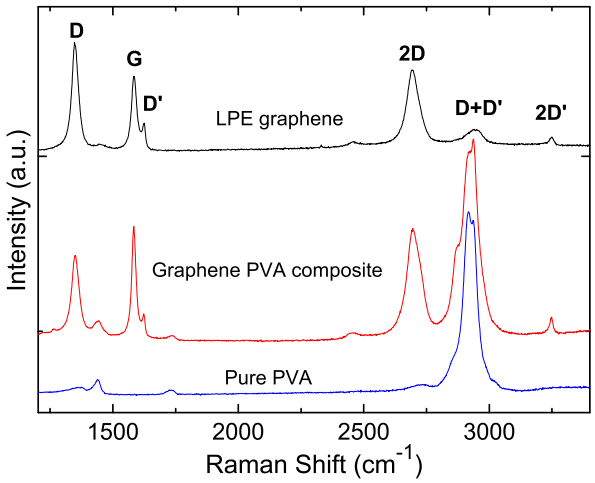

Fig. 1. Raman spectra of flake on Si/SiO_2, polyvinyl alcohol (PVA), graphene-PVA composite.

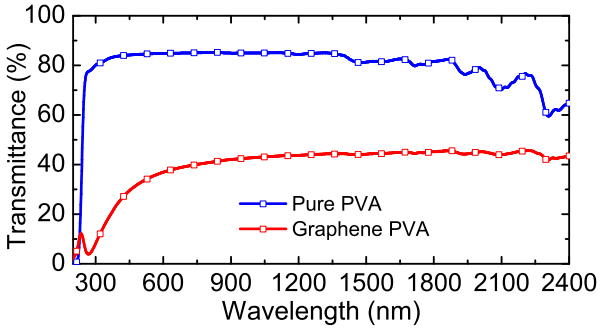

Fig. 2. Transmittance of PVA and graphene-composite.

Figure 2 plots the transmittance of graphene-PVA compared to pure PVA. The UV peak in graphene-PVA is a signature of the van Hove singularity in the graphene density of states [58]. Strong UV absorption is also observed in pure PVA [59]. By considering the pure PVA absorption, we can estimate that of the graphene component to be $\sim$50% in the NIR. Given that a monolayer absorbs $\sim$2.3% [60], we estimate an average $\sim$21 layers cross the light path.

#172887 - $15.00 USD Received 18 Jul 2012; revised 28 Aug 2012; accepted 29 Aug 2012; published 18 Oct 2012

The GSA is then prepared by sandwiching 2 mm^2 of the composite between two fiber connectors, adhered with index matching gel. The integrated device has ∼4 dB (∼60%) total insertion loss.

3. Experimental setup

The laser cavity is schematically shown in Fig. 3. It comprises all-fiber integrated components for an environmentally robust and compact system. A Tm-doped fiber amplifier (TDFA), with integrated optical isolator (ISO), having ∼25 dB small signal gain at 1.94 μm, and a broad gain bandwidth (full width at half maximum, FWHM ∼60 nm) is followed by a fiber pigtailed airgap (∼80% insertion loss) used to include a bandpass filter (BPF) for pulse stabilization, with 80% maximum transmission and 11 nm transmission bandwidth, centered ∼1.94 μm. A fused-fiber output coupler (OC) extracts 10% of the light per pass; a polarization controller (PC) allows adjustment of the intra-cavity polarization. We estimate the overall cavity group velocity dispersion to be -59.7 ps^2 km^{-1}, determined from the solitonic spectral sidebands observed when the oscillator was operating without the bandpass filter that was included to stabilize the pulse train.

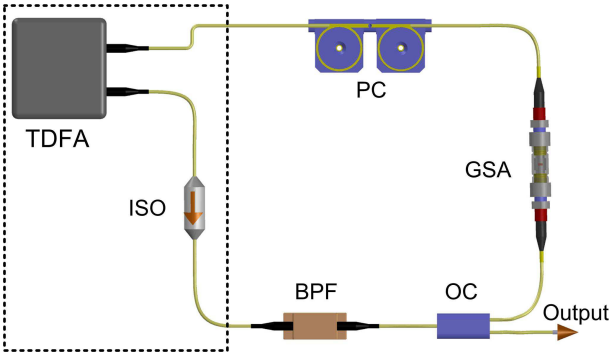

Fig. 3. TDFA-Tm-doped fiber amplifier; ISO-isolator; BPF-bandpass filter; OC-output coupler; GSA-graphene-SA; PC-polarization controller

4. Results and discussion

The autocorrelation of the output pulse, and the corresponding optical spectrum are plotted in Fig. 4. Figure 4(a) shows that the pulse temporal profile is well represented by a $sech^2$. The FWHM duration (after deconvolution) is 3.6 ps. The corresponding FWHM spectral width is 2.1 nm, giving a time-bandwidth product ∼0.59, indicating low chirp [61]. The output power is ∼2 mW. Although the laser operates with negative cavity dispersion, and the pulses are soliton-like, the typical spectral sideband signature of deviation from average soliton operation is not observed, because the soliton length, given by $z_{sol.} = \frac{\pi}{2}\frac{\tau_0^2}{|\beta_2|}$, is long ($z_{sol.} \sim 300$ m) compared to cavity length (31 m $\approx \frac{1}{10} z_{sol.}$), with τ_0 the pulse duration and β_2 the group velocity dispersion.

The stability and quality of the generated pulses are evaluated via the radio frequency (RF) spectrum [62]. Figure 5 plots the fundamental and 60^{th} harmonics over long (1 MHz) and short (8 kHz) frequency spans. The long range spectra indicate that the stability is high, with peak to noise-floor ratio limited by our 300 Hz resolution (the noise floor of the analyzer is plotted in red). No sidebands at harmonic cavity frequencies are observed over the 1 MHz span, suggesting good pulse-train stability and no Q-switching instabilities. This is confirmed

#172887 - $15.00 USD Received 18 Jul 2012; revised 28 Aug 2012; accepted 29 Aug 2012; published 18 Oct 2012

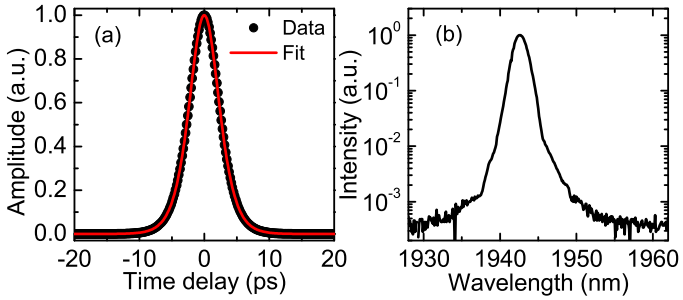

Fig. 4. (a) Autocorrelation, (b) optical spectrum.

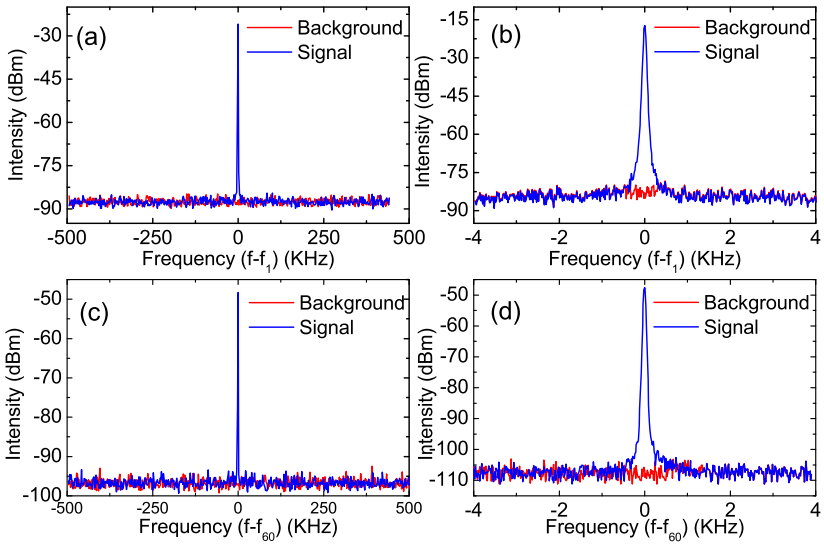

Fig. 5. RF spectra. (a) Fundamental, (c) 60^{th} harmonic on a long range span (1MHz), with 300Hz resolution; (b) Fundamental, and (d) 60^{th} harmonic on a short range span (8kHz), with 30Hz resolution.

by a spectral sweep over 100 MHz, showing the first fifteen harmonics of the fundamental cavity frequency (Fig. 6).

The short range spectra (Fig. 5(b,d)), spanning 8 kHz with 30 Hz resolution, reveal a low level pedestal component $\sim$70 dB from the central f_0 spike. Following Ref. [62], we estimate the energy fluctuations, defined as output pulse energy change divided by average output energy, as $\Delta E = \left[\frac{\Delta P \Delta f}{\Delta f_{\text{Res.}}}\right]^{1/2}$, where ΔP is the power ratio between the central spike at f_1 and the peak of the noise band, Δf (Hz) is the frequency width of the noise component, and $\Delta f_{\text{Res.}}$ (Hz) is the resolution bandwidth of the spectrum analyzer. With $\Delta P = 1 \times 10^{-6}$, $\Delta f = 730$ Hz and $\Delta f_{\text{Res.}} = 30$ Hz, give low pulse-to-pulse energy fluctuation $\Delta E \approx 5 \times 10^{-3}$.

Similarly, when the amplitude noise is low, the timing jitter can be evaluated as [62]: $\frac{\Delta t}{T} = \frac{1}{2\pi n}\left[\frac{\Delta P_n \Delta f}{\Delta f_{\text{Res.}}}\right]^{1/2}$, where T is the cavity period, n is the harmonic order. The low-frequency timing jitter (Fig.5(d)), evaluated at the 60^{th} harmonic with $\Delta P_{60} = 1.6 \times 10^{-5}$, $\Delta f = 393$ Hz and $\Delta f_{\text{Res.}} = 30$ Hz, is estimated as $\Delta t/T = 3.9 \times 10^{-5}$. Given the long cavity period $T = 155$ ns,

#172887 - $15.00 USD Received 18 Jul 2012; revised 28 Aug 2012; accepted 29 Aug 2012; published 18 Oct 2012

this indicates a low timing jitter $\Delta t \approx 6$ ps.

Our analysis suggests that, despite a very simple cavity consisting of non-polarization maintaining (PM) fiber, the laser emits high-quality pulses with low amplitude fluctuations (0.5%) and relatively low timing jitter ~ 6 ps. Although the laser mode-locks without the bandpass filter, the quality of the emitted pulses is compromised, with an increase in the RF noise.

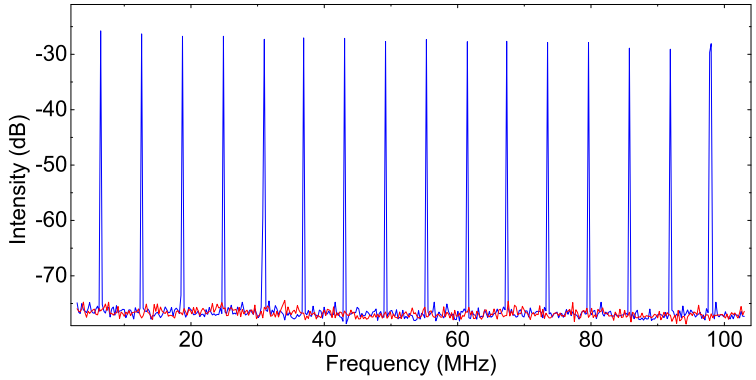

Fig. 6. (Blue) RF spectrum over 100 MHz,with 3 kHz resolution. (Red) analyzer background.

5. Conclusion

In summary, we reported stable continuous-wave mode-locking of a Tm-doped fiber laser, using a graphene-based saturable absorber. The laser generated 3.6 ps pulses at 6.46 MHz, with $\sim$0.4 nJ pulse energy, demonstrating the operation of graphene in the mid-IR. This simple all-fiber design supports low noise operation in a small footprint, suitable for packing in a compact single-unit system. In addition, this ultrafast laser could be realized using all-PM fiber components, which should further improve the stability and noise properties [63].

Acknowledgments

We acknowledge funding from ERC grant NANOPOTS, EPSRC Doctoral Prize Fellowship, EPSRC grant EP/GO30480/1, EU Grants RODIN and GENIUS, a Royal Society Wolfson Research Merit Award, a RAEng Fellowship.

#172887 - $15.00 USD Received 18 Jul 2012; revised 28 Aug 2012; accepted 29 Aug 2012; published 18 Oct 2012